Journal of Computational Design and Engineering 5 (2018) 329–336

Contents lists available at ScienceDirect

Journal of Computational Design and Engineering

journal homepage: www.elsevier.com/locate/jcde

Parameterized Extended Finite Element Method for high thermal gradients

Christian Zeller [a,*], Binu Surendran [b], Micheal F. Zaeh [a]

[a] TUM Department of Mechanical Engineering, Institute for Machine Tools and Industrial Management, Technical University of Munich, Germany
[b] Faculty of Mechanical and Process Engineering, University of Applied Sciences Augsburg, Germany

ARTICLE INFO

Article history:
Received 12 September 2017
Received in revised form 6 December 2017
Accepted 7 December 2017
Available online 7 December 2017

Keywords:
XFEM
Heat equation
Steep thermal gradients
Thermal shocks
Parameterized ansatz functions

ABSTRACT

The Finite Element Method results in inaccuracies for temperature changes at the boundary if the mesh is too coarse in comparison with the applied time step. Oscillations occur as the adjacent elements balance the excessive energy of the boundary element. An Extended Finite Element Method (XFEM) with extrinsic enrichment of the boundary element by a parameterized problem-specific ansatz function is presented. The method is able to represent high thermal gradients at the boundary with a coarse mesh as the enrichment function compensates for the excessive energy at the element affected by the temperature change. The parameterization covers the temporal change of the gradient and avoids the enrichment by further ansatz functions. The introduced parameterization variable is handed over to the system of equations as an additional degree of freedom. Analytical integration is used for the evaluation of the integrals in the weak formulation as the ansatz function depends non-linearly on the parameterization variable.

1. Introduction

Simulation is no longer just for the generation of process understanding (Langermann, 2008). Nowadays, it is used as an integral element in the development process and by this reduces production costs (Gausemeier et al., 2013). However, it is crucial that the simulation is capable of correctly modeling the major factors of influence. In processes with laser sources, steep temporal and spatial thermal gradients occur at the boundary as a consequence of the high local energy input. In addition, the load-time at which a point is subjected to the laser spot can be extremely short due to the laser speed, e. g. in the magnitude of 1 m/s for laser beam melting (King et al., 2015). In a thermomechanical analysis it is important to determine the temperature field correctly in order to obtain the real warping behavior. Due to the short-term occurrence of the heat input, the Finite Element Method (FEM) requires a very fine mesh in the region affected by the laser beam in order to fulfill the *penetration depth condition* and simulate the thermal gradients with sufficient accuracy. The disregard of the penetration depth condition will result in spatial oscillations of the solution and a violation of the maximum principle of the heat equation (Hogge & Gerrekens, 1983). Using FEM, the number of required degrees of freedom leads to a high computational effort. Otherwise, a correct physical representation of the occurring thermal gradient cannot be achieved.

A method for the efficient calculation of steep thermal gradients at the boundary is presented which avoids the usage of a fine spatial discretization. Instead of mesh refinement, the affected elements are locally enriched by a parameterized problem-adjusted shape function, where the parameterization-variable is treated as an additional degree of freedom. This allows not only the representation of the sharp gradient at a time but also of its temporal behavior. The nonlinear dependency of the enrichment function from the parameterization variable requires an analytical integration.

The outline of the paper is as follows. Section 2 provides an overview of methods for avoiding fine local discretization. The concept of the Parameterized Extended Finite Element Method is introduced in Section 3. The results are presented in Section 4. Discussions and conclusions are made in Section 5.

2. State of the art for high thermal gradients

The heat equation, also known as Fourier equation, is a second order quasilinear partial differential equation. The general homogeneous form is

$$c(T)\rho(T)\frac{\partial T(x,t)}{\partial t} = \nabla \cdot [\lambda(T)\nabla T(x,t)] \quad \forall x \in \Omega, t \in [0, t_M] \tag{2.1}$$

with the temperature dependent material parameters thermal conductivity λ, density ρ and specific heat capacity c.

Peer review under responsibility of Society for Computational Design and Engineering.
* Corresponding author.
E-mail address: christian.zeller@iwb.mw.tum.de (C. Zeller).

https://doi.org/10.1016/j.jcde.2017.12.001
2288-4300/

Internal heat sources are neglected as only temperature changes resulting from boundary conditions are considered in this paper. Additionally, only isotropic material ($\boldsymbol{\lambda} = \lambda$) is regarded. The heat equation requires initial and boundary conditions to be a well-posed problem and to obtain a unique solution. For the sake of simplicity and without loss of generality, only Dirichlet boundary conditions are considered and units are not indicated in the paper as the dimensionless form is used in the following.

In most cases it is not possible to find an analytical solution for the partial differential equation in (2.1). Therefore, the equation is weakened to a more general form which must be fulfilled for only certain test functions $\psi(x) \in V$. Additional transformation by Green's function results in the following form:

$$\int_\Omega c(T)\rho(T)\frac{\partial T}{\partial t}\psi \, d\Omega + \int_\Omega \lambda(T)\nabla\psi \cdot \nabla T \, d\Omega = 0 \tag{2.2}$$

The Finite Element Method discretizes the region Ω into n nodes $x_1, \ldots, x_n$ and approximates the temperature T by ansatz functions $\varphi(x) \in W$:

$$T(x,t) = \sum_{k=1}^{n} T_k(t)\varphi_k(x) \tag{2.3}$$

with T_k the nodal temperatures at the nodes x_k. The same ansatz functions φ are used for the temperature T as well as for test functions ψ. By including this approximation in (2.2) the following system of equation is obtained:

$$M(T) \cdot \dot{T} + S(T) \cdot T = 0 \tag{2.4}$$

with

$$M(T)_{ij} = \int_x c(T)\rho(T)\varphi_i\varphi_j \, dx \tag{2.5a}$$

and

$$S(T)_{ij} = \int_x \lambda(T)\frac{\partial\varphi_i}{\partial x}\frac{\partial\varphi_j}{\partial x} \, dx \tag{2.5b}$$

exemplary for the one-dimensional case. A more detailed derivation can be found in (Zienkiewicz & Taylor, 2002).

The region Δx affected by a change in the boundary condition after the time Δt can be expressed by the penetration depth condition. It reads as follows for the heat equation with constant material parameters:

$$\Delta x \leqslant k\sqrt{\frac{\lambda}{\rho c}\Delta t}, \quad k \in \mathbb{R}^+ \tag{2.6}$$

The value of k differs due to the kind of boundary condition (Hogge & Gerrekens, 1983; Yan, 2002). In order to obtain a correct solution without oscillation a sufficient fine mesh is required inside the penetration depth. (Hogge & Gerrekens, 1983) uses four elements for the discretization of the penetration depth. Fewer elements result in oscillation and thereby violation of the maximum principle (Fig. 2.1). Several approaches exist with the aim to avoid the required fine mesh in the simulation of thermal processes with high gradients. They will be presented in the following.

The most convenient procedure is the adaptive refinement of the mesh. The elements in the region of interest are subdivided into smaller elements. However, this is not effective for every kind of element. In order to overcome this problem, structural meshes are used and automatically refined with a predefined refinement strategy (Pal et al., 2016). The disadvantage is that a structured mesh can only be obtained for simple geometries or if inaccuracies in the geometric fidelity of the mesh are accepted.

The discrete maximum principle is one of the basic characteristic properties of classical solutions of second order partial differential

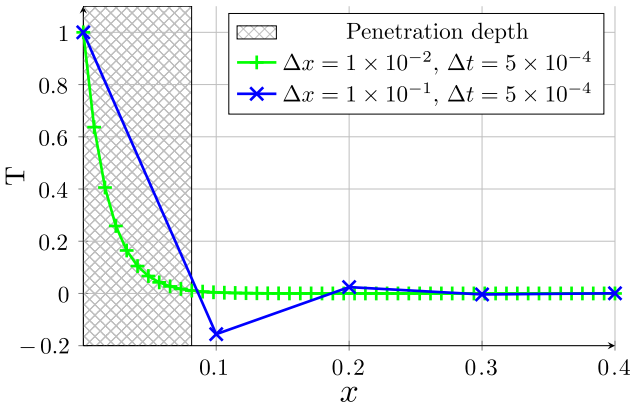

Fig. 2.1. Comparison of FEM results that meet (green) and violate (blue) the penetration depth condition of Eq. (2.6).

equations (Zienkiewicz & Taylor, 2002). It is satisfied in the FEM procedure by obtaining the system matrix of the discretized domain in the M-matrix form. An M-matrix, an invertible matrix A with elements $a_{ii} > 0, a_{ij} \leqslant 0$ and $A^{-1} > 0$, ensures that the results obtained are physically relevant and consistent, e. g. heat energy flow from a node at higher temperature to the colder one and not vice versa. (Fachinotti & Bellet, 2006) discuss about the work of other authors whose proposed methods provide the required M-matrix form of the system matrix and point out the drawback of the method, wherein the constraints on the geometry of the element restrict the use of general meshing approaches used by FEM software.

The diffusion split method introduces an augmented conductivity λ^*

$$\lambda^* = \lambda\frac{\Delta t_{pd}}{\Delta t} \qquad \text{if} \qquad \Delta t_{pd} > \Delta t \tag{2.7}$$

and the accompanying stiffness matrix S^* in order to compensate for the time step size and satisfy the penetration depth condition for a given value of Δx and the associated Δt_{pd} from Eq. (2.6) (Fachinotti & Bellet, 2006). An appropriate time step is obtained by an iterative process until the unrealistic temperature spikes are reduced in the solution. This method is not pursued further as it involves changing of the governing equations. Also, in case of unstructured meshes, the calculation of Δt_{ts} becomes difficult due to the different element sizes.

The FEM is based on approximating the problem using a piecewise differentiable polynomial, which is incapable of representing steep gradients with a too coarse mesh. The mentioned adaptive refinement of the mesh can be further complicated by the need of updating the topology of the mesh with each new step. This means that when using the conventional mesh refinement approach of the FEM, especially in a transient problem, the process becomes tedious (Khoei, 2015). The Extended Finite Element Method (XFEM) is achieved by enriching the FEM in the domain of interest with special shape functions which are capable of representing high gradients in an efficient manner. XFEM provides a way to obtain accurate results without changing the mesh topology at the nodes near discontinuities or refinement near singularities. (Abbas, Alizada, & Fries, 2010) use a set of four enrichment functions to cover the total change of the thermal gradient over time. The domain $\Omega =]0, 1[$ was discretized by 10 elements and the obtained accuracy by the XFEM was several orders of magnitudes greater than by the FEM. Nevertheless, in order to obtain the optimal set of enrichment functions a previous optimization run is necessary.

The presented Parameterized XFEM avoids the enrichment by several functions and the a priori determination of those. The

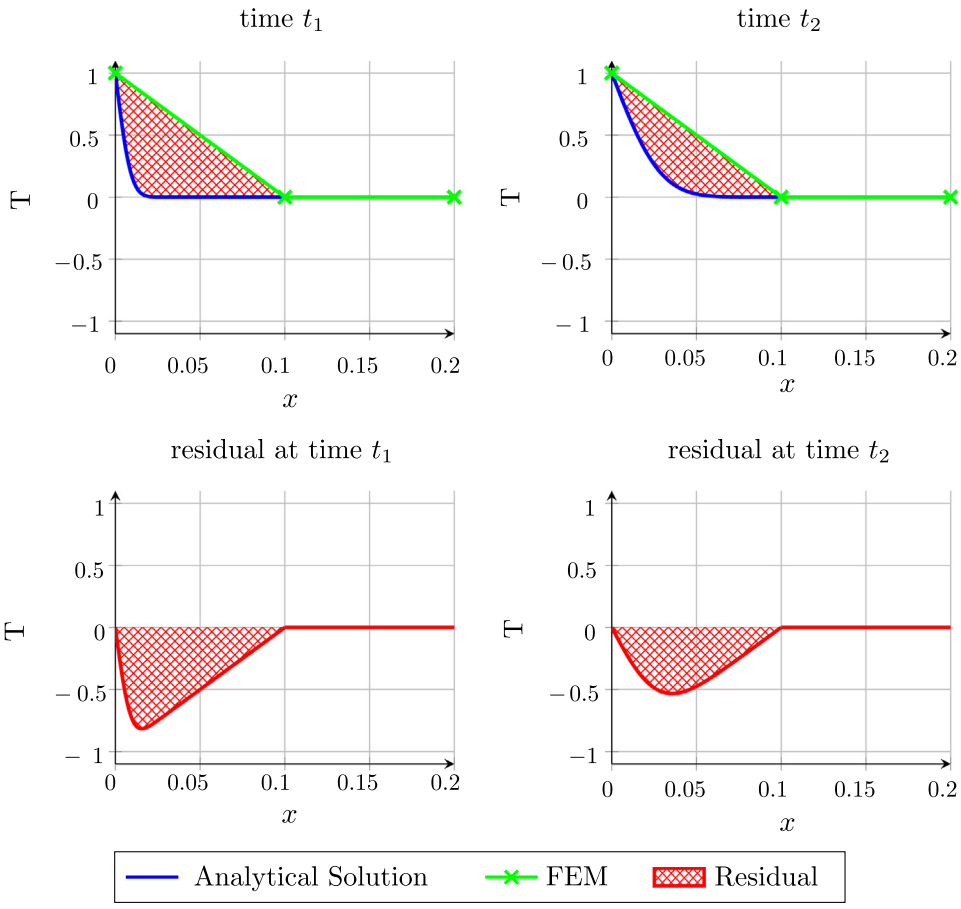

Fig. 3.1. Assumed remaining residual by FEM with correct nodal values at time t_1 and $t_2, t_1 < t_2$.

FEM is enriched by a parameterized function and the optimal parameter is simultaneously calculated for every time step with the calculation of the thermal field.

3. Parameterized Extended Finite Element Method

The Finite Element Method tries to correctly map the energy input from the boundary condition even if the ansatz functions are not able to represent the gradient in a sufficient manner. Thus, the surrounding elements compensate for the excessive energy in the boundary element and consequently oscillations occur as shown in Fig. 2.1.

Fig. 3.1 shows the remaining residual over the time, assuming that the FEM determines the correct node values. The analytical solution for the semi-infinite heat equation serves as a reference since it can be used for short-term problems in bounded domains, too (Polifke & Kopitz, 2009):

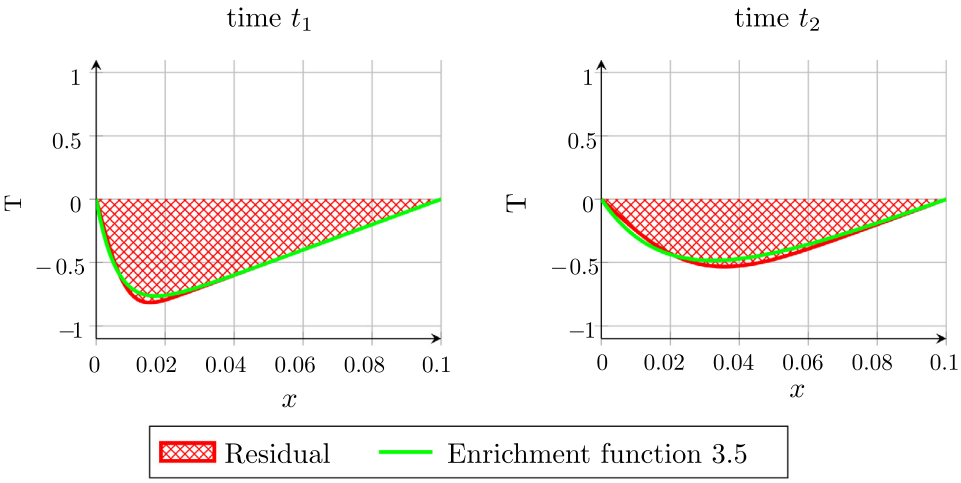

Fig. 3.2. Approximation of the residuals from Fig. 3.1 by the enrichment function (3.5) at time t_1 and $t_2, t_1 < t_2$.

$$T_{ana}(x,t) = 1 - \operatorname{erf}\left(\frac{x}{\sqrt{4at}}\right), \quad a = \frac{\lambda}{\rho \cdot c} \tag{3.1}$$

The aim of the presented method is to *extrinsically* enrich for the excess energy in the boundary element and to reduce the energy imbalance which leads to oscillations or inaccuracies. The enrichment functions φ^*_{ij} disappear on the boundary and are only intended to compensate the remaining residual per element (Fig. 3.1, below) as the FEM delivers the correct node values. Additionally, the enrichment function is parameterized in order to cover the residual change over time. The parameterization variable ζ is handed over to the system as an additional degree of freedom and is calculated simultaneously to scale the gradient. Consequently, an initial value of ζ is necessary for a well posed problem. The value is significant for the required accuracy since it sets the initial gradient.

3.1. Formulation

The PARAMETERIZED EXTENDED FINITE ELEMENT METHOD for the enrichment of m elements in one dimension is thus given by

$$T^*(x,t) = \sum_{k=1}^{n} T_k(t)\varphi_k(x) + \sum_{(i,j)\in\Lambda} \left[T_i(t) - T_j(t)\right]\varphi^*_{ij}(x, \zeta_{ij}(t)) \tag{3.2}$$

where $\Lambda, |\,\Lambda\,| = m$ is a set of pairs (i,j) with i and j being the indices of adjacent nodes of the enriched elements.

The Eq. (3.2) is included in (2.2) similar to the FEM and the following system of equations is obtained:

$$M(T^*, \dot{T}^*) + S(T^*) = 0 \tag{3.3}$$

with

$$M(T^*, \dot{T}^*)_k = \int_x c(T^*)\rho(T^*)\dot{T}^*\phi_k \, dx \tag{3.4a}$$

$$S(T^*)_k = \int_x \lambda(T^*)\frac{\partial T^*}{\partial x}\frac{\partial \phi_k}{\partial x} \, dx \tag{3.4b}$$

and $\phi_k \in \left\{\varphi_j, j = (1,\ldots,n)\right\} \cup \left\{\varphi^*_{ij}, (i,j) \in \Lambda\right\}$.

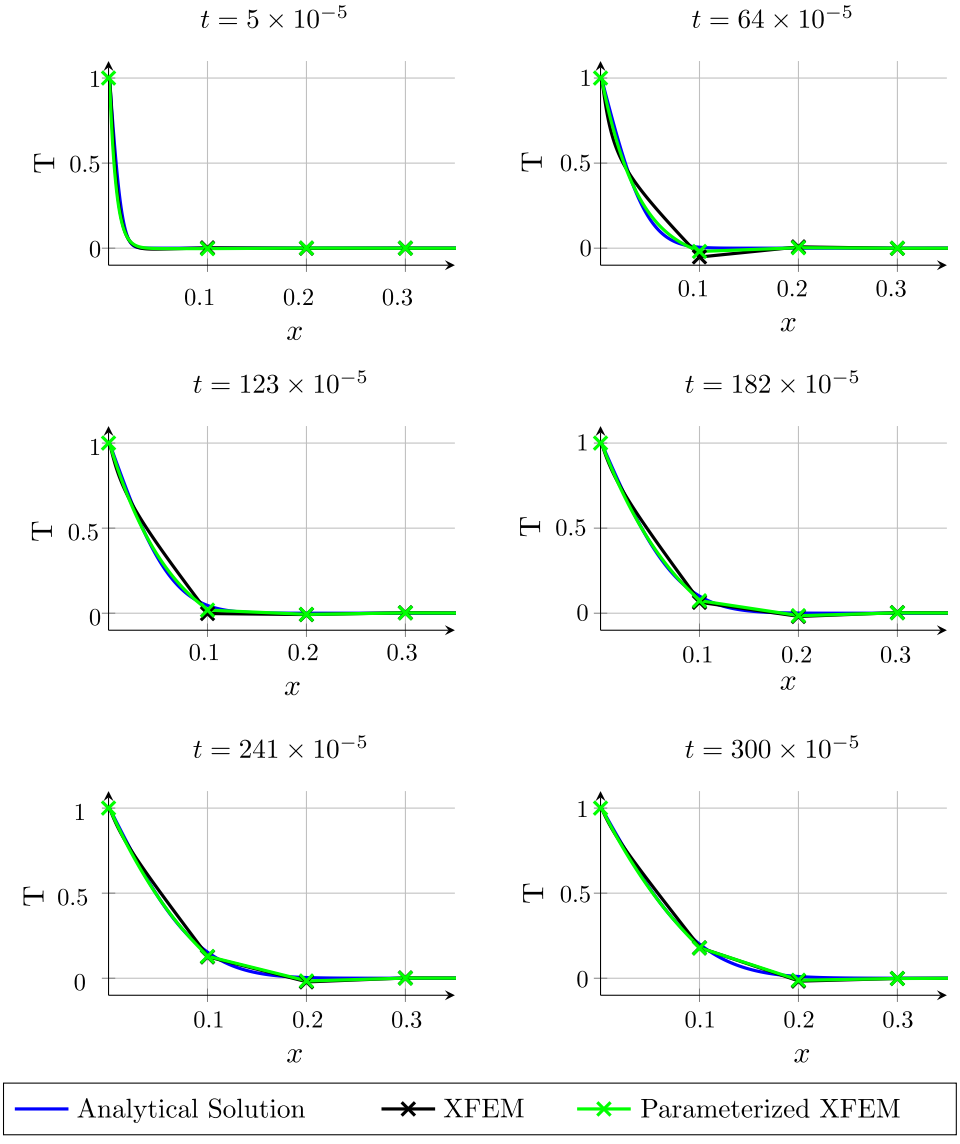

Fig. 4.1. Results for the Parameterized XFEM and the XFEM with enrichment of the first element. A constant time steps was used and a total number of 300 time steps were done.

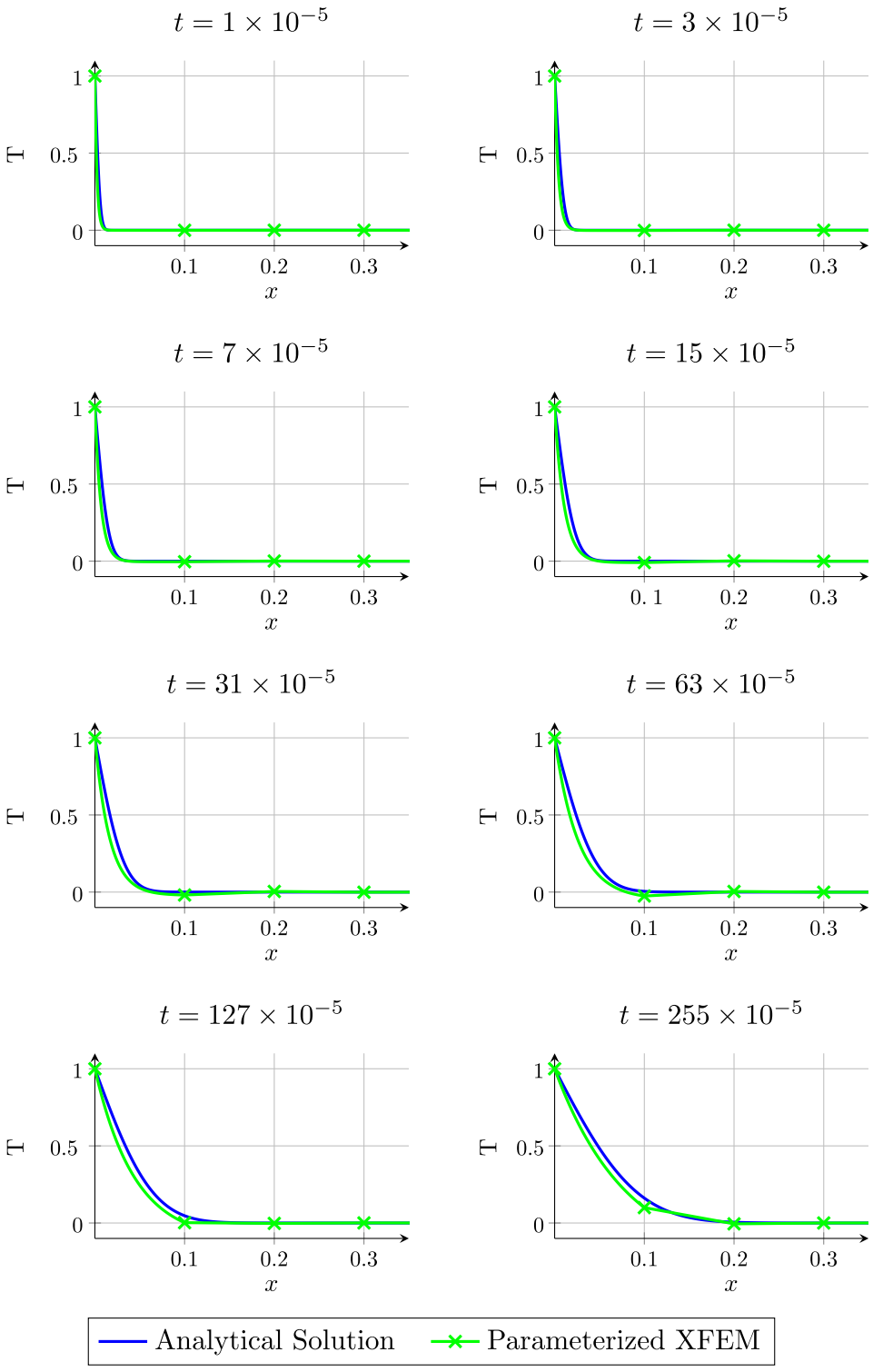

Fig. 4.2. Results for the Parameterized XFEM with enrichment of the first element and a quadratic time step adaption, i. e. $\Delta t_{i+1} = 2\Delta t_i$. A total number of 8 time steps were done.

3.2. Enrichment functions

The inability of standard linear FEM is overcome by using enrichment functions which can approximate the residual in (3.1) and represent high gradients in combination with the standard shape functions from the FEM. These functions can be, for example, exponential functions, trigonometric functions or Gaussian error functions (e. g. $\exp(\zeta - \zeta x), 1 - \mathrm{erf}(\zeta x)$). In order to obtain a suitable enrichment function for the Parameterized XFEM, the linear portion is subtracted as it is already covered by the FEM shape function. In addition, the function is scaled to vanish on the boundary of the element. Exemplary enrichment functions are

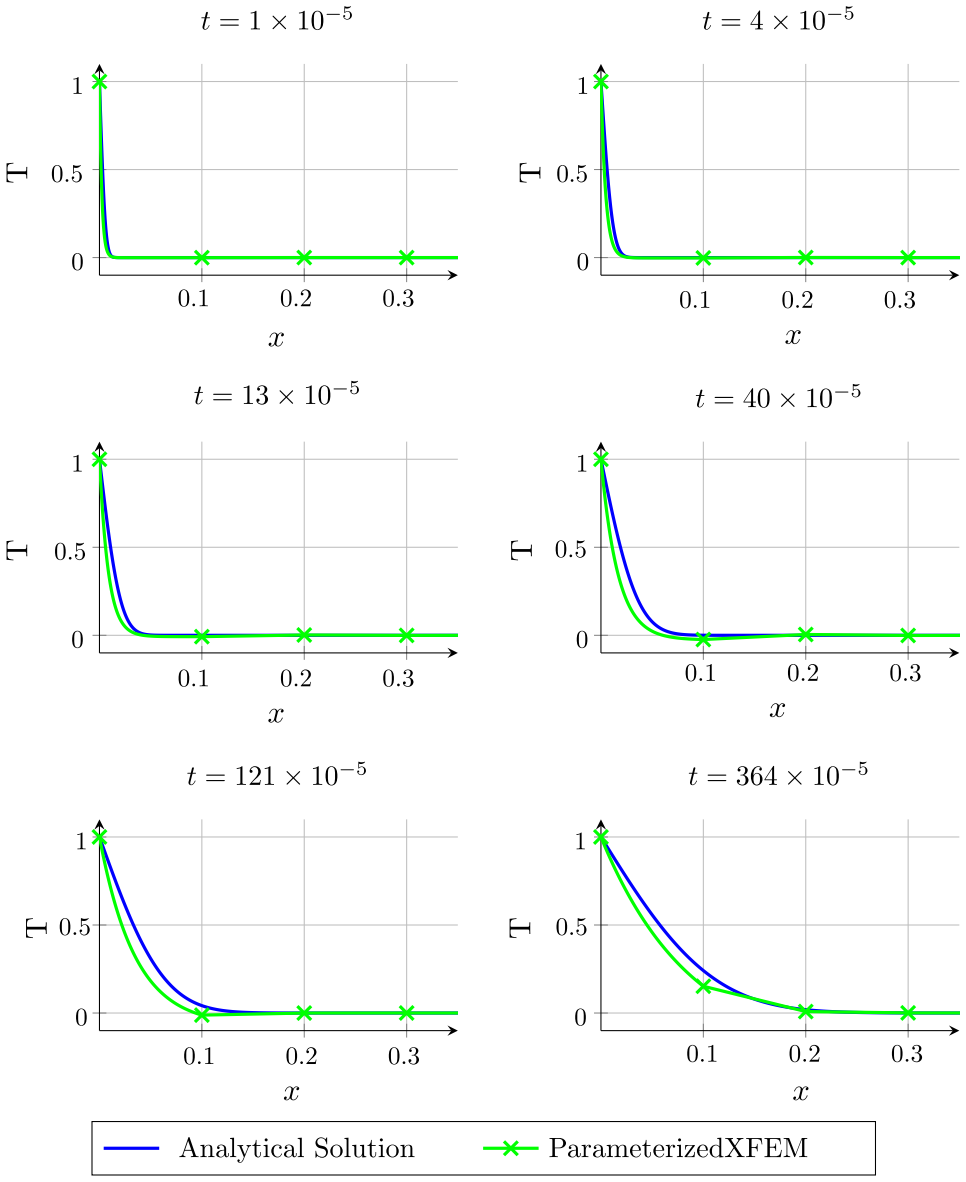

Fig. 4.3. Results for the Parameterized XFEM with enrichment of the first element and a cubic time step adaption, i. e. $\Delta t_{i+1} = 3\Delta t_i$. A total number of 6 time steps were done.

$$\varphi^*(x,\zeta) = \frac{\exp(\zeta - \zeta\frac{x}{h}) - 1}{\exp(\zeta) - 1} - \left(1 - \frac{x}{h}\right) \tag{3.5}$$

or

$$\varphi^*(x,\zeta) = \frac{\operatorname{erf}(\zeta h) - \operatorname{erf}(\zeta x)}{\operatorname{erf}(\zeta h)} - \left(1 - \frac{x}{h}\right) \tag{3.6}$$

$$\operatorname{erf}(x) = \frac{2}{\sqrt{\pi}} \int_0^x e^{-\tau^2} \, \mathrm{d}\tau \tag{3.7}$$

Fig. 3.2 shows the possible approximation of the remaining residual from Fig. 3.1 by the enrichment function (3.5).

The enrichment by the Gaussian error function according to (3.6) promises a high degree of accuracy as it is directly derived from the analytical solution (3.1). Although the use of the Gaussian error function is not practicable because of the inherent integral in the formulation which has to be calculated at every step and thus makes the formulation costly. Hence, it will not be considered in the following and only the parameterized enrichment function (3.5) is analyzed.

3.3. Quadrature

Similar to the FEM, the integrals in Eq. (3.4) have to be determined in order to obtain the global system of Eq. (3.3). The dependency of the enrichment function from the additional parameterization variable ζ_{ij} is non-linear in contrast to the temperature values T_k. Therefore, the evaluation of the integrals in (3.4) cannot be decoupled from ζ_{ij} as it is done for T_k in the FEM.

The claim of the presented method is the use of parameterized shape functions, whose additional parameter ζ_{ij} is able to cover a large temporal range of the gradient, i. e. $\zeta_{ij} = \mathcal{O}(1-10)$. For this reason, static quadrature rules with fixed integration points are not applicable. On the other hand, adaptive quadrature formulas slow down the assembly of the global system of equations as additional optimization runs are necessary. Therefore, the integrals in Eq. (3.4) are analytically solved.

Numerical integration schemes are generally used in the FEM, but there are also approaches to solve the integrals analytically (Videla, Baloa, Griffiths, & Cerrolaza, 2008). Those approaches have the aim to save computational effort in the simulation. Neverthe-

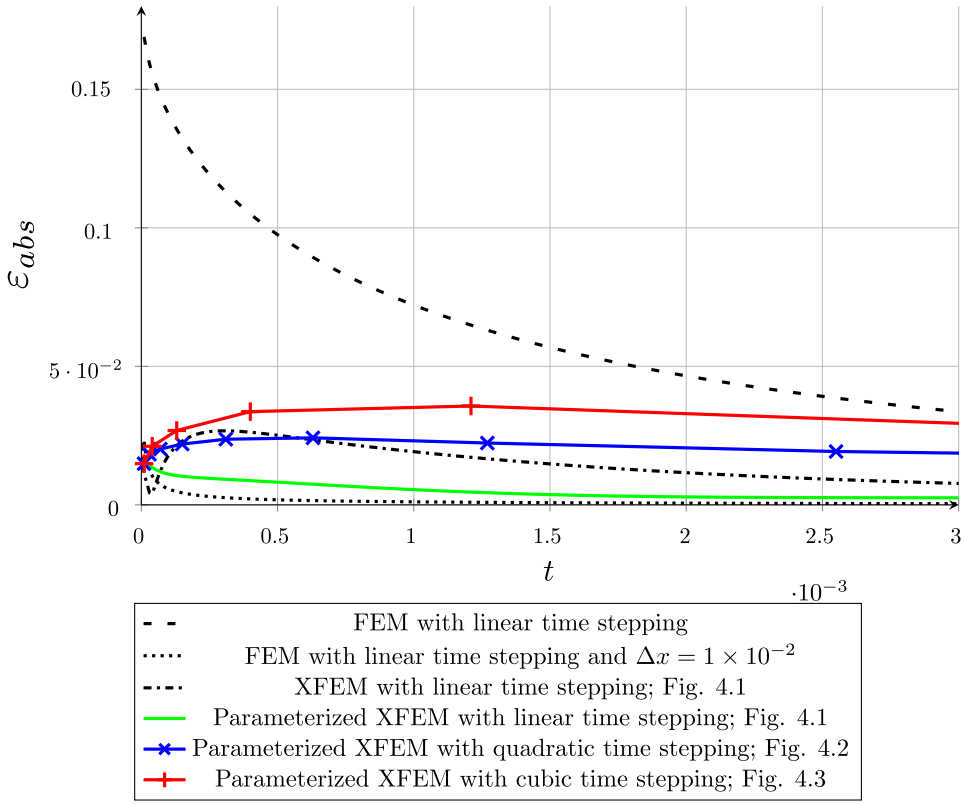

Fig. 4.4. Absolute spatial error ε_{abs} over time evaluated for the enriched element at the left boundary.

less, the exact determination of the integrals is not required for convergence (Zienkiewicz & Taylor, 2002).

4. Results

The method was implemented for the homogeneous linear heat equation in one dimension

$$\frac{\partial T(x,t)}{\partial t} = a\frac{\partial^2 T(x,t)}{\partial x^2} \quad \forall x \in [0,1], t \in [0,t_M] \tag{4.1}$$

with the boundary and initial conditions

$$T(0,t) = 1, \quad \forall t \in [0,t_M], \tag{4.2a}$$
$$T(1,t) = 0, \quad \forall t \in [0,t_M], \tag{4.2b}$$
$$T(x,0) = 0, \quad \forall x \in [0,1]. \tag{4.2c}$$

The thermal diffusivity a was chosen to be 1. The domain $[0,1]$ was discretized in 10 elements of first order and enriched by the parameterized enrichment function from Eq. (3.5) at the boundary element on the left side. The value $\zeta_{1,2}(0) = 100$ was chosen as additional necessary initial condition for the parameterization variable. The implicit Euler was used as numerical integrator and the Newton method solves the resulting system of equations.

The method is dedicated for short-term heat problems where only the boundary element is affected by the temperature change in the first time step and the penetration depth condition (Eq. (2.6)) is largely violated. Therefore, the first time step was chosen to be $\Delta t_0 = 1 \times 10^{-5}$ due to the element size $\Delta x = 1 \times 10^{-1}$ and the period of observation was restricted to the temperature change of the first two elements, i. e. $t_M \approx 3 \times 10^{-3}$ with the penetration depth value k from (Yan, 2002). The domain was assumed to be semi-infinite since the maximum considered Fourier number was

$$Fo = a\frac{t_M}{2\Delta x} = 7.5 \times 10^{-2} \tag{4.3}$$

and the analytical solution T_{ana} of the semi-infinite heat equation was thus used for validation (Polifke & Kopitz, 2009, p. 319).

The results for the Parameterized XFEM with constant time steps and the analytical solution are shown in Fig. 4.1. Only the first three elements are plotted since the remaining elements are not affected by a temperature change during the period of observation. In addition, the results for the conventional XFEM are provided. The similar enrichment function (3.5) was used for the XFEM as for the Parameterized XFEM. In contrast to the Parameterized XFEM, the boundary element was enriched by three functions with the constant values $\zeta = 100, 15$ and 5 to cover the change of the gradient over time. The comparison with the FEM is omitted as it was already shown in Fig. 2.1 that the FEM leads to non-usable results when the penetration depth condition is violated.

The use of constant time steps is usually an unnecessary computing effort. Hence, the Parameterized XFEM was also applied to quadratic and cubic time step schemes. The results are shown in Figs. 4.2 and 4.3.

The absolute spatial error is shown in Fig. 4.4 and was evaluated using the following definition:

$$\varepsilon_{abs}(t) = \|T^* - T_{ana}\|_2 = \left(\int_0^{\Delta x} [T^*(x,t) - T_{ana}(x,t)]^2\, dx\right)^{\frac{1}{2}} \tag{4.4}$$

All simulations were performed using MATLAB and the Symbolic Math Toolbox (MATLAB, 2016).

5. Discussion & conclusion

The conventional XFEM is able to decrease the error in comparison to the FEM with similar element size. However, the error fluctuates. This is because the XFEM correctly obtain the temperature only for certain points in time when the solution can be approximated by just one enrichment function. However, the transition of the temperature field of these points in time is nonlinear while

the XFEM can only linearly represent it. Therefore, the error increases between these certain points and the maximal error strongly depends on the choice of the constants ζ in (3.5). It was shown that the Parameterized XFEM, with ζ as additional degree of freedom, is able to determine a solution with an absolute error less than 1.5×10^{-2} and without fluctuation. A element size of a magnitude smaller is required for the FEM in order to obtain comparable results.

The Parameterized Extended Finite Element Method overcomes the inability of the FEM to correctly map the energy input with a too coarse mesh. The appearing steep gradient at the boundary can be represented with sufficient agreement by the enrichment function and oscillations at adjacent nodes are avoided. The temporal change of the gradient takes place with only one additional parameter. The refinement of the mesh or the enrichment by further ansatz functions is not necessary.

As it can be seen in Fig. 4.4, an adaptive time stepping method should be used since the uniform adaption of the time steps initially leads to an increase in the absolute error. However, this was not the focus of this paper and should only provide the transferability of the method to adaptive time stepping methods.

The concept of parameterized enrichment functions can be applied to further problems and is not restricted to the heat equation.

Conflict of Interest

Authors declare that there is no conflict of interest.

Acknowledgment

This project has received funding from the Clean Sky Joint Undertaking under the European Union's Seventh Framework for research, technological development and demonstration Programme under grant agreement number 714246.

References

Abbas, S., Alizada, A., & Fries, T.-P. (2010). The XFEM for high-gradient solutions in convection-dominated problems. *International Journal for Numerical Methods in Engineering, 82*(8), 1044–1072. https://doi.org/10.1002/nme.2815.

Fachinotti, V. D., & Bellet, M. (2006). Linear tetrahedral finite elements for thermal shock problems. *International Journal of Numerical Methods for Heat & Fluid Flow, 16*(5), 590–601. https://doi.org/10.1108/09615530610669120.

Gausemeier, J., Czaja, A., Wiederkehr, O., Dumitrescu, R., Tschirner, C., & Steffen, D. (2013). Studie: Systems engineering in der industriellen praxis. In M. Maurer, S.-O. Schulze (Eds.), *Tag des Systems Engineering, Carl Hanser Fachbuchverlag, s.l.* (pp. 113–122).

Hogge, M., & Gerrekens, P. (1983). Steep gradient modelling in diffusion problems. In R. W. L ewis, K. Morgan, & B. A. Schrefler (Eds.). *Numerical methods in heat transfer* (Vol. 2, pp. 73–98). John Wiley & Sons.

Khoei, A. R. (2015). Extended finite element method: Theory and applications. In *Wiley series in computational mechanics*. https://doi.org/10.1002/9781118869673.

King, W. E., Anderson, A. T., Ferencz, R. M., Hodge, N. E., Kamath, C., Khairallah, S. A., & Rubenchik, A. M. (2015). Laser powder bed fusion additive manufacturing of metals; physics, computational, and materials challenges. *Applied Physics Reviews, 2*(4), 041304. https://doi.org/10.1063/1.4937809.

Langermann, R. (2008). *Beitrag zur durchgängigen Simulationsunterstützung im Entwicklungsprozess von Flugzeugsystemen*. Braunchweig <http://www.digibib.tu-bs.de/?docid=00026819>.

MATLAB and Symbolic Math Toolbox. (2016). Version 9.1.0.441655 (R2016b), The MathWorks Inc., Natick, Massachusetts.

Pal, D., Patil, N., Kutty, K. H., Zeng, K., Moreland, A., Hicks, A., ... Stucker, B. (2016). A generalized feed-forward dynamic adaptive mesh refinement and derefinement finite-element framework for metal laser sintering—part ii: Nonlinear thermal simulations and validations 2. *Journal of Manufacturing Science and Engineering, 138*(6), 061003. https://doi.org/10.1115/1.4032078.

Polifke, W. & Kopitz, J. (2009). Wärmeübertragung: Grundlagen, analytische und numerische Methoden, 2nd ed., Ing-Maschinenbau, Pearson Studium, München u.a. <http://lib.myilibrary.com/detail.asp?id=505990>.

Videla, L., Baloa, T., Griffiths, D. V., & Cerrolaza, M. (2008). Exact integration of the stiffness matrix of an 8-node plane elastic finite element by symbolic computation. *Numerical Methods for Partial Differential Equations, 24*(1), 249–261. https://doi.org/10.1002/num.20274.

Yan, X. (2002). On the penetration depth in fourier heat conduction. In *8th AIAA/ASME joint thermophysics and heat transfer conference* (pp. 1–7). doi:https://doi.org/10.2514/6.2002-2881.

Zienkiewicz, O. C., & Taylor, R. L. (2002). *The finite element method* (5th ed.). Oxford: Butterworth-Heinemann.